

# ***RF-Sim: a Treatment Planning Tool*** **for Radiofrequency Ablation of Hepatic Tumors**

Caroline Villard, Luc Soler, Nicolas Papier, Vincent Agnus,  
Afshin Gangi, Didier Mutter and Jacques Marescaux  
IRCAD - 1, place de l'Hôpital - F67091 STRASBOURG - France  
caroline.villard@ircad.u-strasbg.fr  
www home page: <http://www.ircad.org/>

## **Abstract**

*With recent advancements of technology, radiofrequency ablation has become one of the most used techniques to treat liver tumors. But radiologists still have to face the difficulty of planning their treatment while only relying on 2D slices acquired from CT-scan. We present in this paper a tool called RF-Sim, being part of a complete 3D reconstruction and visualization project, and including both a realistic radiofrequency ablation simulator for training and rehearsal, and an automatic treatment planner taking into account tumor's environment. They help radiologists to have a better visualization of patients anatomic structures and pathologies, and allow them to easily find an adequate treatment. They run on a common laptop and can be used in the operating room.*

## **1. Introduction**

In the past few years, new minimally invasive techniques emerged as an alternative for the treatment of unresectable liver tumors. These techniques also have the advantage to be lighter for the patient than classic surgery. Among them, radiofrequency (RF) ablation is considered as one of the easiest, safest, and most predictable [5]. It consists in a tumor denaturation, caused by the emission of radiofrequency from the tip of a needle-like probe that heats and causes necrosis of the cancerous cells.

The success of RF treatments relies on 3 main criteria: a maximum volume of eliminated cancerous cells, a minimum volume of healthy tissue damaged, and the choice of secure trajectories for needle insertions. However, the planning of such a treatment is still difficult for radiologists that can only rely on 2D scanner slices. That is why recent techniques of scanner image reconstruction were developed to help radiologists in having a better 3D visualization of

their patients anatomy [10], and improving the information at their disposal remain a topical subject of research.

After a brief state of the art, we describe how we developed a system based on the 3D view of patients organs, that allow to realistically simulate needle placement, and lesion growth. Then, we will explain the second functionality of our system, that is the automatic planning of needle positions, optimizing the criteria. We will particularly put the accent on the last criterion, the choice of trajectories avoiding vital organs, that is the most recent improvement. Before concluding, we will expose some of our significant results.

## **2. State of the art**

Recent published studies and measurements showed a direct relationship between several anatomic, pathologic, or technical factors and lesion size and shape. Most of these factors influence lesion size: the model of generator supplying power [3], blood supply occlusion [9], a cirrhosis of the liver [4]. Another major factor rather influences lesion shape: the "heat-sink effect" is due to the presence of large vessels ( $\varnothing > 2mm$ ) and results in a cooling of the surrounding zone, reducing the benefits of the RF treatment in this area. All these factors have to be taken into account for an accurate RF ablation simulation.

On the technical aspect, until now very few developments have been carried out in the domain of RF ablation simulation and planning. A few studies concern other minimally invasive treatments such as cryotherapy [8], or are centered on finite elements modeling and does not seem to be real time [11]. T. Butz proposed a very interesting cryotherapy simulator and planner, included in *3D-Slicer*, that can also be extended to one type of RF probe [1]. However, it can only compute the best positioning of cryoprobes within a predefined window of the body, and does not take into account the presence of surrounding organs.

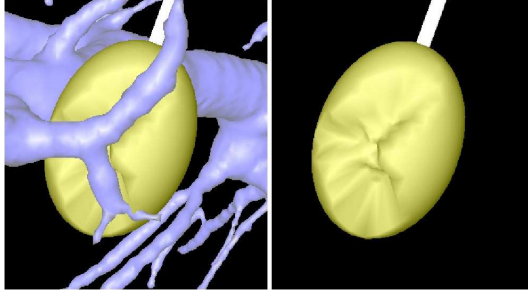


**Figure 1. Deformation of the necrosis zone due to the presence of surrounding vessels**

### 3. Simulation of the necrosis zone

In response to a need from radiologists to improve patients anatomy visualization and treatment planning, our researches led to the development of a tool called *RF-Sim*. This tool makes the link between 3D reconstruction of slices obtained from an enhanced spiral CT scan, using an automated algorithm described in [10], and a 3D viewer and virtual treatment simulator.

A user can visualize and manipulate the 3D scene representing a patient’s organs, he can add and place one or several probes, and see the predicted lesion simulated as a meshed spheroid, and then he can freely move and rotate it to see the updated lesion. Indeed, to take into account the heat-sink effect, the lesion is deformed by “repulsing” its vertices according to the proximity of a vessel. If the user moves the probe, the lesion is updated in real time. This method and obtained results are detailed in [12]. An illustration is presented on Fig.1.

This simulator allows the radiologist to rehearse, to try various scenarios before the treatment, and to immediately see what will be the effects of these needles placements according to tumor location, shape and size. The real-time aspect of our simulator allows it to be run on a common laptop, being able to be carried and used in the operating room.

### 4. Automatic treatment planning

The previous realistic lesion simulation functionality is complemented by an automatic needle placement planning system, that helps radiologists in finding an optimal treatment strategy. This is done using 2 functions. One function computes, for a fixed location and orientation of a needle, the minimal spheroid containing the tumor plus its additional security margin (mandatory to prevent local recurrence of a tumor after treatment [2]). The second minimizes the volume resulting from the first function by trying other

locations and orientations, progressively converging to an optimal situation. To ensure a total burning of the whole volume of the tumor and its margin, we use the voxel representation of the shape to include.

The first one is a quite simple algorithm, that we called *ComputeBestSize*, based on a simplification of ellipsoid fitting. Indeed, the lesions we mesh are particular spheroids with radii  $r_1$ ,  $r_2$ , and  $r_3$  verifying:  $r_3 = r_1$  and  $r_2 = k.r_1$ , where  $k$  is the following ratio:  $\{major\ axis\ size\} / \{minor\ axis\ size\}$ . The algorithm then computes the smallest  $r_1$  allowing every voxel of the tumor and margin shape to be inside the spheroid defined by the equation  $\frac{x^2}{r_1^2} + \frac{y^2}{k^2 r_1^2} + \frac{z^2}{r_1^2} = 1$ . The returned result is the volume of the spheroid  $V = \frac{4}{3}\pi k r_1^3$ . This algorithm is generalized for the treatment of larger or multiple tumors by several needle insertions, and then is called *ComputeBestSizeMoreSpheroids*: we sort tumor shape voxels according to their nearest needle tip, and each subset of voxels will be included their own spheroid. The volume obtained in return is the total volume of the spheroids. This step is illustrated on Fig.2(a) and (b).

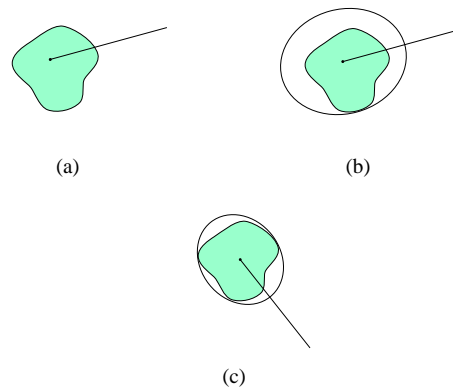


**Figure 2. (a) and (b): fitting an ellipse with fixed center and orientation around a 2D shape; (c): fitting a minimal ellipse around a 2D shape**

The second algorithm, called is an adaptation of one of the classical minimization methods, Downhill Simplex method [7]. The value to minimize is the volume obtained from algorithm 1. Parameters are the location and orientation of the needle, with a precision used as the stopping criterion. Starting from an initial simplex for the parameters, composed of the initial position given by the user and a weighting of unit vectors, the initial simplex contracts itself into a valley floor after a few iterations, and returns an optimized position. We also tried other minimization methods, such as Powell’s direction set method, or simulated annealing algorithm, but with less efficient results in terms of volume size and execution time. This algorithm

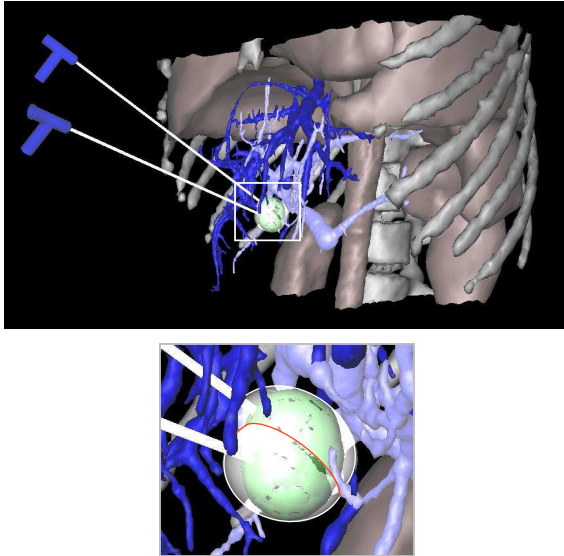


**Figure 3. Minimization of the burning zone using 2 overlapping spheroids**

is also extended for multiple needle placements, by simply increasing the number of vertices in the simplex. An example of a result is shown on Fig.3 where 2 overlapping spheroids, whose placement were found automatically, minimally cover a tumor.

## 5. Taking into account surrounding organs

The previous section described how we compute optimized placements for consecutive needle insertions, maximizing volume of burnt cancerous tissue, and minimizing affected healthy tissue. This responds to the two first criteria of a successful treatment, but the third one is still to be considered.

For now, a minimal spheroid including tumor and margin shapes is found, but we still do not take into account surrounding organs, and the trajectories we recommended may still pass through bones or gallbladder for instance. To have an appropriate prediction of the optimal trajectory to follow, we have to avoid all trajectories that would go through vital or rigid organs.

First of all, we have to determine what kind of trajectory has to be avoided. A trajectory is acceptable only if it intersects skin, liver, and a tumor and its margin. All trajectories intersecting other organs are forbidden, either because a needle insertion through them would be fatal, or cause serious damages (heart, portal vein, etc.), or because their physical properties do not allow a needle to go through (bones). Therefore, for each considered trajectory, we need to compute its intersections with the patients organs.

### 5.1. Intersection between needle and organ

Let us recall that we want our prototype to run on a common laptop, so we have some efficiency requirements that compels us to simplify the computations. Therefore, we chose to replace the needle by a simple segment. That way, the intersection computation is quicker, and can be performed by a simple line/mesh intersection algorithm.

To speed up even more the process, we chose to take advantage of the graphic cards by using an accelerated picking to compute the intersections. A customized picking function, derived from rendering techniques, allows us to cast a ray from the origin of the needle and following its direction, and to obtain in return a sorted list of all touched organs, with the depth of the intersections. We only keep intersections located between the origin and the tip of the needle. This part of the process is as fast and robust as the rendering of one part of the scene, that is accelerated by every 3D graphic card.

We parse the intersections list, and we eliminate intersections with skin, liver, and tumor shape and margin. Then, if one or more intersections persist, it means that the considered trajectory is not secure and has to be avoided. This is illustrated on Fig.4, where the left scheme is acceptable because needle only crosses skin, liver, and tumor and its margin, but right scheme shows a wrong trajectory because needle also crosses a bone.

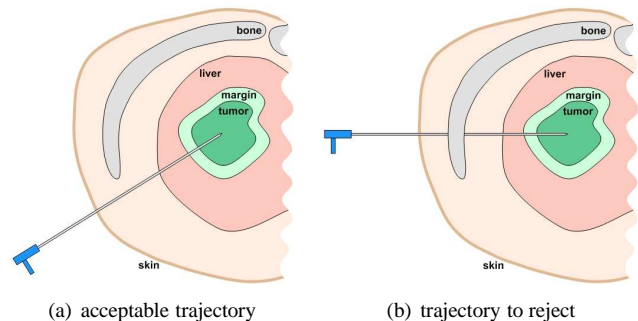


**Figure 4. Finding intersections between organs and needle**

### 5.2. Treatment planning preserving vital organs

Once this intersection computation function is established, we have to include it as a part of the optimization process.

We chose to use the result of the unwanted intersections research as a condition to weigh the volume returned by *ComputeBestSizeMoreSpheroids*. If the trajectory is wrong, this function will return such a high volume that the op-

timization function will necessarily decide to give up progression in this direction and search for a more secure path.

Practically talking, if the needle, for the lesion of which we are going to compute the best size, is going to cross a forbidden organ, then we do not perform the best volume computation, and we place instead as a volume a very high value, prohibitive enough for the optimization process. That way, we save time as many of the tried trajectories will not need a fitting computation, and the time used to compute intersections will be more or less compensated.

### 5.3. Results

A series of experiments was performed on 9 patients cases, whose data came from the Strasbourg Civil Hospital. These tests included 7 small single tumors ( $< 10mL$ ), 1 large single tumor needing 2 needle insertions, and 1 multiple tumor. These multiple tumors are considered as one with several connected components, each of them needing a separate needle insertion. Table 1 summarizes the results of these experiments.

For each patient case, we detailed the number of connected components and the total volume of the tumor (plus additional margin). This tumor information is followed by information on the lesions predicted by the optimization process in two cases: with or without the use of intersection tests. For each of these two categories, we specified both the predicted volume, and the associated percentage  $\{volume\ of\ tumor\} / \{burnt\ volume\}$ . The last data represents the loss of efficiency induced by the introduction of the intersection tests.

**Table 1. Resulting volumes of minimizations (in mL) with and without intersection test**

case	tumor(s)		lesion(s)					loss of percent.
	nb	volume	nb	volume with no collision	effi c. of burn	volume with collision	effi c. of burn	
1	1	7.4	1	10.6	69.8%	11.7	63.2%	6.6%
2	1	6.5	1	10.1	64.3%	10.5	61.9%	2.4%
3	1	5.2	1	8.8	59.1%	10.3	50.5%	8.6%
4	1	2.1	1	2.9	72.4%	3.7	56.7%	15.7%
5	1	3.1	1	3.8	81.6%	3.9	79.5%	2.1%
6	1	4.1	1	5.8	70.7%	6.4	64.1%	6.6%
7	1	3.7	1	4.5	82.2%	4.6	80.4%	1.8%
8	1	18.7	2	21.6, 15.4	n.c.	16.7, 18.5	n.c.	n.c.
9	2	6.9	2	3.4, 6.7	61.1%	3.5, 6.8	67%	1.3%

These results lead us to the conclusion that even if there is a loss with the addition of the collision test, this loss does not seem to be so detrimental, as the average is 5.6%, and the worst loss is 15.7%, and all efficiency percentages remain above 50%. We notice that the smallest losses mainly concern tumors located far away from the vessel network, and close to the skin, while largest losses are encountered

on tumors located deep inside vessel network, or in a central position in the body, surrounded by organs. This point confirms that, the proximity of a complicated shape such as the vessel network decreasing the range of possible trajectories, it is more difficult to find a satisfactory position for the needle; but this difficulty would have also been encountered if the planning was made manually.

We also have to take these results cautiously, as the experiments were performed on patients reconstructions in 3D that did not include stomach and intestine, because the automatic reconstruction part of the project is not yet designed to recognize these organs. Therefore, the results may change for the patients whose tumor is located right behind the intestine when we will have these additional organs at our disposal. Nevertheless, we can even so conclude that our study totally reached one of its goals: we can automatically find trajectories avoiding given vital organs and bones, and giving results that have the smallest possible reduction of efficiency in terms of burnt volume. Obviously, stomach and intestine reconstructions will always have to be available when we will use our prototype in routine, in order to have correct trajectories.

Another point of comparison between the processes with and without intersection test is the execution time. A comparative table is presented below.

**Table 2. Execution times (in sec.) with and without intersection test**

case nb.	time w/ inter. test	time w/o inter. test
1	9	45
2	4	16
3	6	20
4	1	22
5	7	29
6	4	33
7	5	32
8	115	260
9	32	101

On this table, we can see that the intersection tests performed at each iteration of the optimization process noticeably slow it down. The average execution time is 6.5 times slower with intersection tests than without tests. Even if this can still be tolerable for a small tumor such as case #2 (16s.), this increases the duration of the process and can reach prohibitive times when the tumor requires several needle insertions because of its size or its number of connected components. For instance, in our experiments, it takes more than 2 minutes to compute the 2 optimal trajectories to treat a tumor of 18.7 mL, on an Athlon XP 1800+ with 512Mo RAM, and a GeForce3 Ti 200 64Mo. We conclude that

more efforts have to be concentrated on the reduction of the execution time, by optimizing the algorithms.

However, our method is still much faster than T. Butz's algorithm [1], as he announce 15 minutes of computation to place optimally 2 probes, using a 440 Mhz workstation with 512Mo RAM, and only within a small optimization space defined by the radiologists, *i.e.* without taking into account surrounding organs.

Note that a validation process is currently in progress, in collaboration with the Strasbourg Civil Hospital's radiology service. It consists in a preoperative automatic treatment planning, and then a comparison *a posteriori* with the effective treatment in terms of efficiency and accuracy, and will concern in total about 20 patients.

#### 5.4. Discussion and future works

Future works will be focused on two main points: the reduction of the execution time, that is as we said earlier one of the drawbacks of the method, and the improvement of the security and the feasibility of the predicted trajectories.

Indeed, on this second point, we noticed that if the prototype finds a minimal trajectory passing closely between veins through the vascular network, or nearby a vital organ, it will consider this trajectory as being optimal and secure and will return it. However, this may not be the point of view of the radiologist that may consider this trajectory as too risky, because in practice there is a danger of perforation due to imprecisions during the operation. This situation is illustrated on Fig.5.

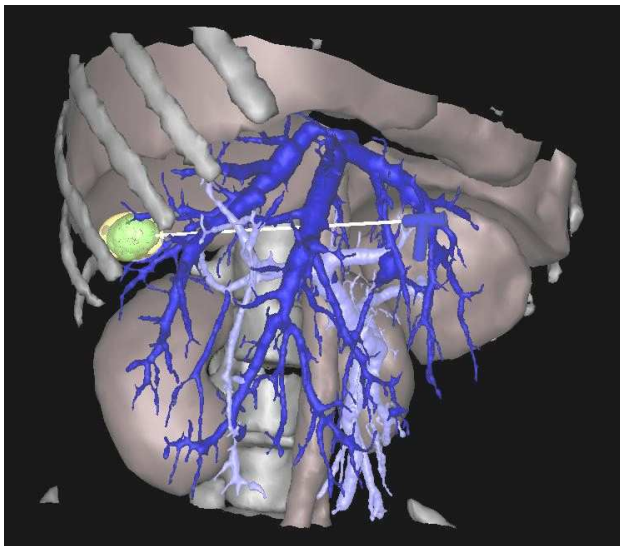


**Figure 5. Trajectory involving major risks**

To avoid this scenario, we plan to use a method derived from the distance transform [6], that is a technique coming from the image processing domain, and that consist in

associating to each point of the 3D space a scalar representing its distance to an organ. It would allow us to compute a distance map for the whole patient's anatomy, to be able to determine for each trajectory the minimal distance to the surrounding organs. That way, we could be warned if a trajectory comes too close to vital structures, and avoid it. Another possibility is to propose the user to choose the sensitivity degree of the tool, by allowing him to modify the parameters of the optimization process with a dialog box. That way, he could define how large is the range for the allowed position and orientation attempts, starting from the initial position he gave. He would have a better control over the zone in which he wishes the needle to be placed. However, this restriction of the research zone would forbid the program to find possibilities in other distant locations.

In a similar idea, another situation is considered by the prototype as a good result, and by the radiologist as an unfeasible scenario: if the needle does not cross any organ except for tumor, margin and liver, it also means that it does not cross the skin, so it may be parallel to the body of the patient (see Fig.6). In that case, the radiologist will not be able to insert the needle following this trajectory. It sometimes occurs because some information is missing about the patient, due to a restriction of the area acquired with the CT scan. To avoid this, we could try to acquire larger zones of the patients, but above all we could impose the trajectory to cross necessarily the skin of the patient. If the scanned zone is not extensive, this could reduce the range of possible trajectories, but in compensation it would avoid impossible ones.

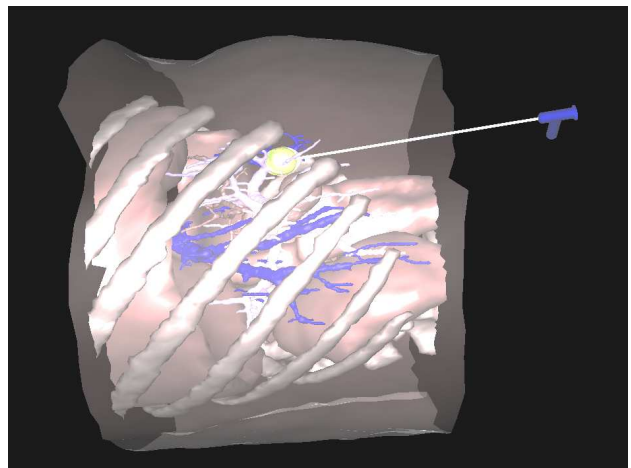


**Figure 6. Trajectory impossible to reproduce in practice**

Some improvements also have to be done as regards to the problem of long execution times. As it seems to us that it would be difficult to accelerate even more the intersec-

tion test function, we have to search other means. We could find a way to avoid testing collisions at every iteration, for instance by using the above mentioned distance transform to create a “risky zone” around each organ, and eliminate quicker large portions of space. We also could try to find other optimization methods, that would be faster than those we have implemented so far (Downhill Simplex, Powell’s conjugate, and simulated annealing methods). Lastly, we could study criteria allowing us to adjust automatically optimization parameters according to tumor location and environment for instance.

## 6. Conclusion

We introduced a tool, called *RF-Sim*, that is part of a whole project allying 3D reconstruction of 2D slices acquired from an enhanced spiral CT-scan, and radiofrequency ablation simulation and planning, within the framework of hepatic tumors treatment.

The simulator part predicts the treatment’s result, given a position and an orientation of the needle, and displays a realistic spheroid representing what would be the necrosis zone according to various surrounding factors. This tool allows the radiologist to have a better visualization of his patient’s anatomy, and to see what would be the efficiency of some treatment strategies. It is aimed to be used as a training and rehearsal tool.

*RF-Sim* also includes an automatic treatment planner, that is able to compute the optimal placement and orientation for a RF needle in order to burn the whole tumor and its security margin, and to preserve healthy tissue and avoid the perforation of vital organs. Our method is based on an intersection function derived from 3D rendering techniques, and relies on the 3D card acceleration.

Both tools use voxel representations of some of the anatomical structures to allow faster computations. Thanks to this, the simulator is real-time, and can be used on every common laptop and be brought in an operating room, and our treatment planning tool is noticeably faster than those developed so far in the domain.

However, some improvements still have to be done, especially to verify if the recommended trajectory is technically feasible, and if it is not too risky for the patient’s vital structures.

## References

- [1] T. Butz, S. K. Warfield, K. Tuncali, S. G. Silverman, E. van Sonnenberg, F. A. Jolesz, and R. Kikinis. Pre- and intra-operative planning and simulation of percutaneous tumor ablation. In *MICCAI*, pages 317–326, 2000.
- [2] B. Cady, R. L. Jenkins, G. D. S. Jr., W. D. Lewis, M. D. Stone, W. V. McDermott, J. M. Jessup, A. Bothe, P. Lalor, E. J. Lovett, P. Lavin, and D. C. Linehan. Surgical margin in hepatic resection for colorectal metastasis: a critical and improvable determinant of outcome. *Annals of Surgery*, 227:566–571, 1998.
- [3] T. de Baere, A. Denys, B. J. Wood, N. Lassau, M. Kardache, V. Vilgrain, Y. Menu, and A. Roche. Radiofrequency Liver Ablation: Experimental Comparative Study of Water-Cooled Versus Expandable Systems. *Am. J. Roentgenol.*, 176(1):187–192, 2001.
- [4] T. Livraghi, S. N. Goldberg, S. Lazzaroni, F. Meloni, L. Solbiati, and G. S. Gazelle. Small hepatocellular carcinoma: Treatment with radio-frequency ablation versus ethanol injection. *Radiology*, 210(3):655–661, 1999.
- [5] J. F. McGahan and G. D. Dodd III. Radiofrequency ablation of the liver: Current status. *American Journal of Roentgenology*, 176(1):3–16, 2001.
- [6] A. Meijster, J. B. T. M. Roerdink, and W. H. Hesselink. A general algorithm for computing distance transforms in linear time, 2000.
- [7] W. H. Press, S. A. Teukolsky, W. T. Vetterling, and B. P. Flannery. *Numerical Recipes in C++: The Art of Scientific Computing (Second Edition)*. Cambridge University Press, 2002.
- [8] J. C. Rewcastle, G. A. Sandison, P. Kennedy, B. J. Donnelly, and J. C. Saliken. 3-dimensional visualization of simulated prostate cryosurgery. In *Soc. Cardiovascular & Interv. Radiology 25th Ann. Meeting*, San Diego, 2000.
- [9] S. Rossi, F. Garbagnati, R. Lencioni, H.-P. Allgaier, A. Marchiano, F. Fornari, P. Quaretti, G. D. Tolla, C. Ambrosi, V. Mazzaferro, H. E. Blum, and C. Bartolozzi. Percutaneous Radio-frequency Thermal Ablation of Nonresectable Hepatocellular Carcinoma after Occlusion of Tumor Blood Supply. *Radiology*, 217(1):119–126, 2000.
- [10] L. Soler, H. Delingette, G. Malandain, J. Montagnat, N. Ayache, C. Koehl, O. Dourthe, B. Malassagne, M. Smith, D. Mutter, and J. Marescaux. Fully automatic anatomical, pathological, and functional segmentation from ct scans for hepatic surgery. *Computer Aided Surgery*, 6(3):131–142, 2001.
- [11] S. Tungjitkusolmun, S. Staelin, D. Haemmerich, J.-Z. Tsai, J. G. Webster, F. T. Lee, D. M. Mahvi, and V. R. Vorprian. Three-dimensional finite element analyses for radio-frequency hepatic tumor ablation. *IEEE Trans. Biomed. Eng.*, 49(2):3–9, 2002.
- [12] C. Villard, L. Soler, N. Papier, V. Agnus, S. Thery, A. Gangi, D. Mutter, and J. Marescaux. Virtual radiofrequency ablation of liver tumors. In *IS4TM (to appear)*, jun. 2003.